be reproduced, even at high-excitation energies. It seems more probable that an intranuclear cascade initiated by high-energy nucleons from (γ, N) processes (such nucleons themselves being strongly forward peaked) is responsible for the high-energy α emission. The cascading nucleons could then eject α particles in a similar reaction mechanism to the (n, α) and (p, α) reactions. Recent work[20] on these (N, α) reactions has yielded a satisfactory explanation of the observed energy spectra, which are similar in form to those observed here. Currently an attempt is being made to interpret our $(e, \alpha)e'$ data in terms of the (N, α) results.

It can be seen from Fig. 1 that the increase in electron energy from 60 to 120 MeV causes an order of magnitude increase in the observed cross section for high-energy α particles ($E_\alpha \sim 18$ MeV). The ratio of virtual-photon intensity at these two energies, for $E_\gamma = 30$ MeV, is 1.6. The high-energy α particles are therefore unlikely to result from a single-step direct reaction mechanism involving the virtual photon.

The authors are grateful to Dr. D. J. S. Findlay for supplying data-acquisition programs and for assistance with the experimental work. We acknowledge the support of the work by the Science Research Council. One of us (J. C. M.) acknowledges the support of the Central Electricity Generating Board; another (A. G. F.) acknowledges receipt of an Edinburgh University Postgraduate Scholarship. We thank Professor W. Cochran for his support and encouragement in this work.

[1]M. Kregar and B. Povh, Nucl. Phys. 43, 170 (1963).
[2]L. Meneghetti and S. Vitale, Nucl. Phys. 61, 316 (1965).
[3]H. Hoffman, B. Prowe, and H. Ullrich, Nucl. Phys. 85, 631 (1966).
[4]N. A. Keller and D. B. McConnell, Can. J. Phys. 50, 1554 (1972).
[5]J. J. Murphy, II, H. J. Gehrhardt, and D. M. Skopik, Nucl. Phys. A277, 69 (1977).
[6]J. L. Matthews, D. J. S. Findlay, S. N. Gardiner, and R. O. Owens, Nucl. Phys. A267, 51 (1976).
[7]S. C. Fultz, R. A. Alverez, B. L. Berman, and P. Meyer, Phys. Rev. C 10, 608 (1974).
[8]I. C. Nascimento, E. Wolynec, and D. S. Onley, Nucl. Phys. A246, 210 (1975).
[9]W. W. Gargaro and D. S. Onley, Phys. Rev. C 4, 1032 (1971).
[10]N. Shikazono and T. Terasawa, Nucl. Phys. A250, 260 (1975).
[11]P. J. Dallimore, Australian National University Report No. ANU-P/512, 1970 (unpublished).
[12]W. Hauser and H. Feshbach, Phys. Rev. 87, 366 (1952).
[13]D. Wilmore and P. E. Hodgson, Nucl. Phys. 55, 673 (1964).
[14]O. F. Lemos, Institute of Nuclear Physics, Université de Paris XI, Orsay, France, Internal Report, Ser. A, No. 136, 1972 (unpublished).
[15]A. Gilbert and A. G. W. Cameron, Can. J. Phys. 43, 1446 (1965).
[16]E. Wolynec, M. N. Martins, and G. Moscati, Phys. Rev. Lett. 37, 585 (1976).
[17]D. H. Youngblood *et al.*, Phys. Rev. C 13, 994 (1976).
[18]V. L. Telegdi and M. Gell-Mann, Phys. Rev. 91, 169 (1953).
[19]P. David, J. Debrus, F. Lübke, H. Mommsen, R. Schoenmackers, and G. Stein, Nucl. Phys. A221, 145 (1974).
[20]M. Blann and A. Mignerey, Nucl. Phys. A287, 301 (1977).

Evolution of Turbulence from the Rayleigh-Bénard Instability

Guenter Ahlers and R. P. Behringer[a]
Bell Laboratories, Murray Hill, New Jersey 07974
(Received 16 January 1978)

Measurements of heat transport through horizontal layers of fluid heated from below are reported for three aspect ratios Γ ($\Gamma = D/2d$, D = diameter, d = height of the cylindrical cells). They show that for $\Gamma = 57$ the fluid flow is turbulent, in the sense that it has an a nonperiodic time dependence, for numbers $R > R_t$ with $R_t \cong R_c$ (R_c is the critical R for onset of fluid flow). For $\Gamma = 4.72$, we find $R_t \cong 2R_c$. For $\Gamma = 2.08$, a quasiperiodic state exists for $R_p \leq R \leq R_t$, with $R_p \cong 10R_c$ and $R_t \cong 11R_c$.

A problem of considerable interest is the manner in which nonperiodic time-dependent flow (turbulence) evolves in a fluid subjected to an external stress.[1-10] We report here on an experimental investigation of this phenomenon in the case of a horizontal fluid layer contained in a cylindrical geometry and heated from below. We find that the sequence of events leading to turbu-

lence is qualitatively altered by changing the aspect ratio $\Gamma \equiv D/2d$ (D = diameter, d = height) of the system. Perhaps most surprising is that for large Γ ($\Gamma = 57$) our results indicate the existence of nonperiodic fluid flow for all temperature differences ΔT larger then the critical value ΔT_c for the onset of convection. For smaller Γ ($\Gamma \cong 5$), there is a range of temperature gradients above ΔT_c for which the fluid flow is time independent, but this range is terminated abruptly by a transition to nonperiodic time-dependent behavior. For even smaller Γ ($\Gamma \cong 2$), we find a transition from time-independent to quasiperiodic flow, followed by a further transition to a nonperiodic state. This latter case has many similarities to the sequence of behaviors observed by others in the case of a rotating fluid (Taylor instability).[4,5]

When a fluid with positive isobaric thermal expansion coefficient α is contained between horizontal parallel plates and heated from below, fluid flow (convection) will occur when the temperature gradient is sufficiently large.[11] A dimensionless measure of the temperature difference ΔT across the cell is given by the Rayleigh number $R \equiv g\alpha d^3 \Delta T/\kappa\nu$, where g is the gravitational acceleration, and where κ is the thermal diffusivity and ν the kinematic viscosity of the fluid. The onset of convection (Rayleigh-Bénard instability) occurs when $R = R_c$, where $R_c = 1708$ for $\Gamma = \infty$. Our measurements were made in three cells of cylindrical symmetry, using normal (i.e., nonsuperfluid) He^4 as the fluid. The cells are identified as A, B, and C and their dimensions together with the relevant fluid properties are given in Table I. Also shown are parameters for cell D, which was used in a previous experiment.[3] All cells had horizontal plates made of copper, which has a thermal conductivity four orders of magnitude greater than that of the fluid. In addition to R, a relevant fluid parameter is the Prandtl number $\sigma \equiv \nu/\kappa$. For the measurements on cells A, B, and D, σ was near 0.8.

For cell C, however, the height was so small that the critical Rayleigh number could be reached only at relatively high temperatures where α is large. In that case σ is also larger. We made measurements at two temperatures, corresponding to $\sigma = 4.40$ and 2.94 (see Table I). In each cell, the effective thermal conductivity (Nusselt number N) of the fluid was measured as a function of R. Results near R_c for cells A, B, and D have been published elsewhere,[12] and for R close to R_c they are in good agreement with theoretical calculations. Our Nusselt numbers for the large-aspect-ratio cell C agree well with the measurements of Koshmieder and Pallas.[13]

The measurements relevant to time-dependent fluid flow states consisted of monitoring the temperature difference ΔT across a cell as a function of time while the heat current $\dot{q}$ through the cell and the temperature at the cold (top) end of the cell were held constant. Typically, 3500 sequential measurements of ΔT, evenly spaced in time, were made for each value of $\dot{q}$. The time interval between measurements depended upon the frequency range of interest, but was between 3 s and 70 s, corresponding to 3 h to 70 h of measurements at a given $\dot{q}$.

In order to characterize the time dependence of ΔT, the power spectral density $P(f)$ was calculated as a function of the frequency f. Typical results at several Rayleigh numbers for cell C ($\Gamma = 57$) with $\sigma = 2.94$ are shown in Fig. 1. The values of R/R_c are given by the numbers adjacent to the curves. The lowest curve, labeled 0.00, represents the experimental noise level obtained with $R < R_c$. The presence of broad-band noise in the spectra for $R > R_c$ shows that ΔT is nonperiodic in time even R/R_c as small as 1.27. In each case, the spectrum has a maximum near zero frequency.

In order to obtain a measure of the frequency scale, we calculated the frequency $f_1 \equiv \int |f| P(f)\, df / \int P(f)\, df$ for each spectrum after correcting for

TABLE I. Fluid properties and dimensions of the convection cells.

Cell	D (cm)	d (cm)	T (K)	ρ (g/cm^3)	λ (erg/sec cm K)	$10^{-7} C_p$ (ergs/g K)	$10^6 \eta$ (P)	$10^4 \kappa$ (cm^2/sec)	$10^4 \nu$ (cm^2/sec)	σ	Γ	d^2/κ (sec)
A	2.502	0.265	2.1841	0.1462	1667	5.05	25.6	2.26	1.75	0.78	4.72	311
B	1.077	0.259	2.1841	0.1462	1667	5.05	25.6	2.26	1.75	0.78	2.08	297
C	2.502	0.022	5.171	0.045	...	...	17.1	0.86	3.80	4.40	57	5.6
			5.444		...	...	17.8	1.35	3.96	2.94		3.6
D	0.926	0.088	4.515	0.1250	2221	5.28	31.1	3.36	2.49	0.74	5.27	23.0

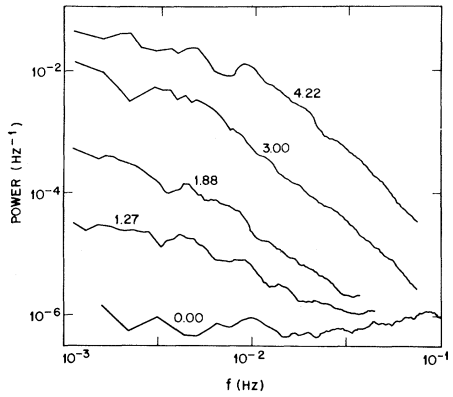

FIG. 1. Power spectral densities, in Hz^{-1}, as a function of frequency in Hz, for $\Delta T/\Delta T_c$ of cell C and $\sigma = 2.94$. The numbers near the curves are the mean values of R/R_c. The spectra have been smoothed over 0.1 decade in frequency.

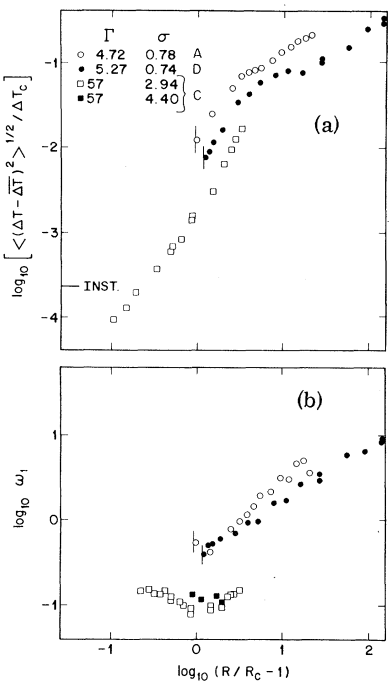

FIG. 2. (a) The rms amplitudes of $\Delta T/\Delta T_c$ for cells A, C, and D, as a function of $R/R_c - 1$, on logarithmic scales. (b) The characteristic frequencies $\omega_1 \equiv \int|\omega|P(\omega)\,d\omega / \int P(\omega)\,d\omega$ of the power spectral densities of $\Delta T/\Delta T_c$ for cells A, C, and D as a function of $R/R_c - 1$ on logarithmic scales.

the instrumental noise level. The corresponding dimensionless frequencies $\omega_1 \equiv (2\pi d^2/\kappa) f_1$ are represented in the lower half of Fig. 2 on logarithmic scales as a function of $R/R_c - 1$ as open squares for $\sigma = 2.94$ and a solid squares for $\sigma = 4.40$. We estimate that ω_1 has an accuracy of 10% or 20% at large R; but at the smallest R the uncertainty in ω_1 may be as large as 50%. The data reveal no systematic dependence of ω_1 upon σ.

A striking feature of the results for ω_1 is their very low values. Although there are no theoretical predictions for the nonperiodic phenomenon which we observed, it may be instructive to make a qualitative comparison with the frequencies calculated for the oscillatory instability by Clever and Busse.[7] Those frequencies are more than two orders of magnitude larger than ω_1 observed for cell C. Thus, the nonperiodic phenomenon which we observe has an extremely slow time scale, and this may be part of the reason why it has not been discovered in previous experiments.[8-10,13]

The open squares in the top half of Fig. 2 are the rms amplitude of the time dependence of $\Delta T/\Delta T_c$ for cell C. Here a correction has been applied for the instrumental noise level which is indicated by the horizontal bar on the left-hand side of the figure. The data demonstrate the existence of time-dependent flow for $R/R_c - 1$ as small as 0.1, and are consistent with an amplitude which remains finite down to R_c and vanishes *at* R_c approximately as $(R - R_0)^{1/3}$. For $R \gtrsim 2R_c$, the dependence of the amplitude upon R is stronger than at smaller R, and is given approximately by $(R - R_c)^2$.

For cell A ($\Gamma = 4.72$) the evolution of time dependence is similar to that reported previously[3] for cell D ($\Gamma = 5.27$). For $R < R_t \simeq 2R_c$, ΔT reaches an equilibrium value which is independent of time within the experimental resolution. For $R > R_t$ the fluid flow is nonperiodic, with spectra which are similar to those for cell C (Fig. 1) in that they have a maximum at $\omega = 0$. For $\omega \gg \omega_1$, we find $P(\omega) \propto \omega^{-n}$ with $n = 4.0 \pm 0.2$.[14] Values of ω_1 for cell A are given as open circles in Fig. 2. Also shown for comparison as solid circles are the previously published results for cell D. Note that the *dimensionless frequencies* for the two cells are very similar to each other, as would be expected since the aspect ratios are so similar. The vertical thermal diffusion times, however, and thus the *actual frequencies*, differ by a factor of 13.5. The rms amplitudes for cells A and D are given in the top half of Fig. 2.

The behavior of cells A and D differs from that of cell C in that the nonperiodic state does not occur until $R_t \simeq 2R_c$. The values of R_t are indicated in Fig. 2 by the small vertical bars at the left-hand ends of the sets of data. At R_t, time

dependence starts with finite amplitude and frequency for cells A and D.

For cell B ($\Gamma = 2.08$), the evolution of the time-dependent states is qualitatively different from that observed in cells A, C, and D. In this case, the fluid flow remains time independent for $R < R_p \simeq 10R_c$.[15] Beyond R_p, a quasiperiodic state evolves with a power spectral density which consists of instrumentally sharp spectral lines. Examples are shown in Figs. 3(a) and 3(b). These spectra contain two frequencies $\omega_a \simeq 1.5$ and $\omega_b \simeq 13.6$, and all other spectral features can be explained as sums and differences of harmonics of ω_a and ω_b. We believe that ω_a and ω_b are incommensurate because they *as well as their ratio* depend mildly upon R. At a well-defined value $R_t > R_p$ broad spectral features appear at nonzero frequencies. An example is shown in Fig. 3(c). At even larger R, the broad-band components completely dominate the spectra, as shown in Fig. 3(d). The behavior observed for this cell has a great deal in common with the results reported for the Taylor instability,[4,5] and for the Rayleigh-Bénard instability with $\Gamma = 3$ and $\sigma = 2.5$ using water as the fluid.[16]

We have seen that the sequence of events leading to nonperiodic (turbulent) flow can be qualitatively altered by changing the aspect ratio of the system. Our largest-aspect-ratio cell, which approximates most closely the laterally infinite system which is attractive to theorists, yielded nonperiodic fluid flow for all experimentally accessible $R > R_c$, and strongly suggests that $R_t = R_c$ for large Γ. Decreasing the aspect ratio tends to suppress the onset of the nonperiodic state, and for $\Gamma = 5$ we obtain $R_t \simeq 2R_c$ with time-independent fluid flow for $R < R_t$. Further decreasing Γ shifts R_t to even higher values, and permits the evolution of a quasiperiodic state prior to the onset of nonperiodic behavior. In this case, when nonperiodicity first occurs, it does so with the power concentrated at nonzero frequencies. This differs from the case of large Γ where nonperiodicity was not preceded by quasiperiodic behavior and where the power spectral density had a maximum at $\omega = 0$. Whereas there are some theoretical models which simulate the behavior observed for small Γ,[1,2,7] the large-Γ behavior observed by us has to our knowledge not yet been discovered on the basis of theory.

We are grateful to J. D. Sieber, A. R. Storm, and B. C. Wonsiewicz for their assistance in putting our automatic data acquisition system into operation.

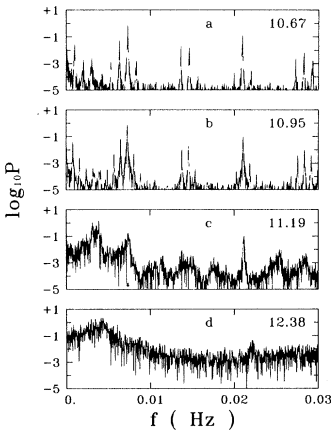

FIG. 3. Power spectral densities, in Hz^{-1}, on a logarithmic scale, as a function of frequency in Hz on a linear scale, for cell B. The numbers in the figures are the mean values of $\Delta T/\Delta T_c$.

[a]Present address: Department of Physics, Wesleyan University, Middletown, Conn. 06547.

[1]For recent reviews, see P. C. Martin, in *Proceedings of the International Conference on Statistical Physics, Budapest, 1975*, edited by L. Pál and P. Szépfalusy (North-Holland, Amsterdam, 1975); P. R. Fenstermacher, H. L. Swinney, S. V. Benson, and J. P. Gollub, in Bifurcation Theory and Applications in Scientific Disciplines, edited by O. Gurel and O. E. Rossler (New York Academy of Sciences, New York, to be published).

[2]J. B. McLaughlin and P. C. Martin, Phys. Rev. Lett. 33, 1189 (1974), and Phys. Rev. A 12, 186 (1975).

[3]G. Ahlers, Phys. Rev. Lett. 33, 1185 (1974), and in *Fluctuations, Instabilities, and Phase Transitions*, edited by T. Riste (Plenum, New York, 1975).

[4]J. P. Gollub and H. L. Swinney, Phys. Rev. Lett. 35, 927 (1975).

[5]R. W. Walden, M. W. Cromar, P. Kittel, and R. J. Donnelly, Bull. Am. Phys. Soc. 21, 1231 (1976).

[6]P. Berge and M. Dubois, Opt. Commun. 19, 129 (1976).

[7]R. M. Clever and F. H. Busse, J. Fluid Mech. 65, 625 (1974).

[8]G. E. Willis and J. W. Deardorff, Phys. Fluids 8, 2225 (1965), and 10, 931 (1967), and J. Fluid Mech. 44, 661 (1970).

[9]F. H. Busse and J. A. Whitehead, J. Fluid Mech. 66, 67 (1974).

[10]R. Krishnamurti, J. Fluid Mech. 42, 309 (1970), and 60, 285 (1973).

[11]See, for instance, S. Chandrasekhar, *Hydrodynamic and Hydromagnetic Stability* (Oxford Univ. Press, Oxford, 1961).

[12]R. P. Behringer and G. Ahlers, Phys. Lett. 62A, 329 (1977).

[13]E. L. Koshmieder and S. G. Pallas, Int. J. Heat Mass Transfer 17, 991 (1974).

[14]For $R \gtrsim 5R_c$, additional structure evolves in the spec-

tral region $\omega >> \omega_1$. This will be discussed in detail elsewhere.

[15]For cell B, a discontinuity in the Nusselt number was observed near $3R_c$. Therefore, in this case we do not expect that the fluid flow for R near R_p and R_t has the circular symmetry observed by Koshmieder and Pallas (Ref. 13).

[16]Fenstermacher *et al.*, Ref. 1.

Positron Annihilation in Indium, Zinc, Cadmium, and Gold in the Temperature Range Down to 4 K

P. Rice-Evans, I. Chaglar, and F. El Khangi
Department of Physics, Bedford College, University of London, Regent's Park, London NW1 4NS, Great Britain
(Received 11 August 1977; revised manuscript received 30 January 1978)

Doppler-broadening measurements have been made on the 511-keV photons resulting from positron annihilation in annealed and plastically deformed samples of indium, zinc, cadmium, and gold. Over the temperature range 4–400 K, distinctive features are observed in each case. Studies with a single crystal of cadmium associate the features with defects at grain boundaries.

Uncertainty surrounds the behavior of positrons in metals at low temperatures. At higher temperatures the trapping model, in which vacancies are assumed to trap positrons, has enjoyed some success; Arrhenius plots and values of vacancy formation energies (E_v) have been reported (for review, see Seeger[1] and West[2]). At intermediate temperatures below the vacancy region, measurements show that the annihilation parameters (for example F, defined in Rice-Evans, Hlaing, and Rees[3]) are a function of temperature; and the original interpretation based on thermal expansions has been challenged by the observation in cadmium of two distinct subvacancy regions,[4] and by models based on phonon-assisted dilatations[4] and self-trapping metastable states.[5] At the Helsingor positron conference, August 1976, a Doppler-broadening study on 99.9999+% pure (6N) annealed indium[6] gave strong support to Seeger's self-trapping model, but controversy reigned. However, subsequently we have failed to find evidence for self-trapping in 5N indium.[7]

As liquid helium temperatures are approached new effects have appeared; in annealed cadmium and gold an unexpected rise in F has been seen at the lowest temperatures,[8] but not in copper.[9,10] In addition, although it has long been known that defects in plastically deformed metals trap positrons,[11] it is only recently that investigations of these phenomena at low temperatures have shown interesting features.

In this Letter we present new Doppler-broadening measurements for a range of temperatures down to 4.2 K. A germanium detector with a resolving power of 1.15 keV at 514 keV has been employed to determine the shape of the 511-keV annihilation γ line. We have used a conventional F parameter[3] defined by the ratio of the number of counts in a chosen central region of the line divided by the counts in the whole line. With this definition, F is linearly related to the number of positrons annihilating with the conduction electrons and hence contributing the narrow parabolic component of the line. Each point in the figures corresponds to a line containing 900 000 counts. Simultaneous measurement of a control ^{103}Ru 497-keV γ ray has been instituted to assess any electronic drift and to allow appropriate correction where necessary. A G parameter, similar in conception to F, was applied to the 497-keV line, and runs corresponding to any significantly low values (rare) were rejected.

The samples were held in a cryostat (<400 K) and a furnace (>300 K), in a vacuum better than 10^{-5} Torr. The temperatures were controlled automatically, and in the cryostat a Au/0.03%-Fe–Chromel thermocouple was used.

Four polycrystalline metals have been studied: indium, zinc, cadmium, and gold. Carrier-free ^{22}NaCl positron sources were evaporated onto the central regions (<5 mm diameter) of two etched specimen disks (diameter >10 mm) which were then pressed in a sandwich configuration. For the annealed samples, the respective purities, disk thicknesses, manufacturers, and annealing conditions were In, 6N, 1.25-mm, Koch-Light, 8 h at 398 K plus 13 h at 373 K, 10^{-5} Torr; Zn, 5N, 1.0 mm, Johnson-Matthey, 8 h at 633 K, 10^{-5} Torr; Cd, 1.6 mm, 99.9996%, Johnson-Matthey, 23 h at 514 K, 10^{-6} Torr; Au, 0.75 mm, 5N, Koch-Light, 21 h at 1000 K, 10^{-6} Torr.

Defects were introduced into the metals by plas-